Progress In Electromagnetics Research M, Vol. 106, 139–152, 2021

Analyzing Effects of Satellite Attitude and Speed Errors on Ocean Current Retrieval for a Doppler Scatterometer

Yuanjing Miao[1, 2], Xiaolong Dong[1, 2, *], and Di Zhu[1]

Abstract—Doppler-based techniques for ocean current measurement have been demonstrated in the past years. The Doppler shift of the ocean backscattering from space-borne microwave instruments not only includes the contributions from ocean current but also includes satellite movement and the wind-wave induced. Geometrical Doppler shift induced by satellite movement is highly dependent on the accuracies of satellite attitude determinations and speed. In this study, we derive the detailed formulas to investigate how satellite attitude determination and speed errors affect ocean current retrieval for a Doppler scatterometer through the spatial correlation coefficient phase and the transformation between orbital coordinate system and satellite-carried local level frame (LLF). Our results show that ocean current speed retrieval accuracy is sensitive to the accuracies of satellite attitude determination and speed, and compared with the satellite speed error, satellite attitude error has a larger impact on ocean current retrieval. By comparisons, with the same attitude accuracy for satellite roll, pitch, and yaw, ocean current speed error induced by the roll error is found to be the smallest. With an accuracy of 0.001° satellite attitude determination and 0.01 m/s for satellite speed accuracy, the total ocean current speed retrieval error induced by satellite attitude determinations (including roll, pitch, and yaw) and speed errors reaches a maximum value of 16.37 cm/s at side-looking direction and a minimum value of 11.05 cm/s at forward and backward-looking directions. Our results confirm the importance of satellite attitude determination accuracy for future ocean current mission and will also be useful to motivate the design of future Doppler measurement instruments.

1. INTRODUCTION

Ocean current plays an important role in atmosphere-ocean exchanges in heat, energy, and flux. High-accuracy and high-resolution ocean current measurement will enhance and improve our understanding of atmosphere-ocean systems [1, 2]. Doppler-based techniques for ocean current measurement have been demonstrated in the past years [3–6]; however, at present, there are no ocean current vector observations from space at a global scale. Recently, new concepts for direct ocean current vector measurement have been proposed, such as SKIM (Sea Surface Kinematics Multiscale Monitoring, SKIM), WaCM (Winds and Currents Mission, WaCM), OSCOM (Ocean Surface Current Multiscale Observation Mission, OSCOM) [6–8]. Doppler scatterometer is a new promising instrument for simultaneous wind vector and ocean current vector measurements at a global scale with wide swath (> 1000 km), while synthetic aperture radar (SAR) system has limited swath that cannot achieve a rapid global coverage [6]. Doppler shift from space-borne microwave radar measurements includes the contributions from satellite movement, the wind-wave induced, and ocean current itself. The geometrical Doppler shift induced by satellite motion is relatively large as the satellite speed is larger than 7 km/s in space depending on the orbital height while most of the ocean current speed magnitude is in the order of several to

Received 6 August 2021, Accepted 2 December 2021, Scheduled 21 December 2021
* Corresponding author: Xiaolong Dong (dongxiaolong@mirslab.cn).
[1] Key Laboratory of Microwave Remote Sensing, National Space Science Center, Chinese Academy of Sciences, Beijing 100190, China. [2] University of Chinese Academy of Sciences, Beijing 100049, China.

hundreds of cm/s. Therefore, to accurately retrieve ocean current, Doppler shift contributions from the satellite movement and wind-wave induced must be accurately removed from the total Doppler shift of ocean surface. It means that the accuracies of Doppler shift estimations of satellite motion and wind-waves contribution directly determine the accuracy of ocean current retrieval. Many studies about the wind-wave induced Doppler shift have been published recently [9–14], and it has been found that the wind-wave induced contribution is highly dependent on ocean state. However, the effect of the accuracy of Doppler shift of satellite motion induced on ocean current retrieval has not been well investigated. The geometric Doppler shift induced by satellite motion can be estimated using the real-time satellite platform attitude and speed information; however, it requires a very accurate and precise measurement of satellite attitude and speed information [3, 4, 15, 16], thus, the accuracies of satellite attitude determination and speed would inevitably affect the ocean current retrieval accuracy.

Ocean surface current vector measurement is still in its early stage, there are few open literatures which specifically investigate the satellite attitude determination and speed errors on ocean current retrieval. In addition, due to the different radar systems (SAR, Doppler scatterometer, and altimeter), the specific methodologies or algorithms to analyze the effects of satellite attitude determination errors on ocean current retrieval are quite different from one radar system to another. For example, in [15], the authors emphasize the necessity of accurate correction of bias caused by geometrical Doppler shift prediction errors for their ocean current retrieval using advanced synthetic aperture radar (ASAR) data. The root-mean-square errors of the Doppler shift after bias correction are found to be 4.7 Hz for VV polarization, which corresponds to a horizontal Doppler velocity of 0.23 m/s. In [17], the authors have considered the error induced by satellite attitude determination and speed errors as one of the sources of the radial velocity error model in their proposed ocean current retrieval method. They found that ocean current speed error induced by satellite attitude determination error could be as large as 0.25 m/s for a Ku-band scatterometer with an accuracy 0.002° of satellite attitude determination. In [6], the authors evaluate the error budget that satellite attitude error induced on the geometrical Doppler shift and point that a specific algorithm is required to stabilize and decrease the platform attitude error for their Ka-band radar altimeter system. A very strict satellite platform stability of 10^{-4} is required to ensure an acceptable radial velocity error. All these studies highlight the great importance of accuracy of satellite attitude determination on ocean current retrieval. However, all the above analyses are aimed at the specific radar systems, and the methods they proposed are not suitable for our proposed Doppler scatterometer [5]. It is very desirable and necessary to investigate the specific effects of satellite attitude determinations and speed errors on ocean current retrieval for our radar system.

In this paper, we mainly focus on investigating the effects of satellite attitude (roll, pitch, and yaw) determinations and speed error on ocean current retrieval for a Doppler scatterometer proposed in [5]. The architecture of the methodology adopted in this study is shown in Figure 1.

As shown in Figure 1, the inputs of the methodology we adopted in this study include satellite attitude determination and speeds errors, and the radar system parameters combining with the corresponding observation geometry. The outputs (shown in the blue dashed boxes) are incidence angle and observation azimuth errors induced by satellite attitude determination errors and ocean current speed error induced by satellite attitude determination and speed errors. The inputs and outputs are linked by the theoretical knowledge (shown in the red dashed boxes).

Following the framework of the methodology, the paper is arranged as follows. Theoretical background knowledge (including the principle descriptions and transformation between orbital coordinates and satellite-carried LLF) is presented in Section 2. The analyses of effects of satellite attitude determinations and speed error induced on ocean surface current, which involves the detailed formula derivation, are shown in Section 3, and the paper is closed with the summaries and conclusions in Section 4.

2. THEORETICAL BACKGROUNDS

The accuracy of ocean current retrieval is determined by the accuracies of interference phase, Doppler model, and satellite attitude determination and speed, where the satellite attitude determination and speed errors affect ocean current retrieval though the variance of phase of spatial correlation coefficient. In this section, we give a principle theoretical description on how satellite attitude determination

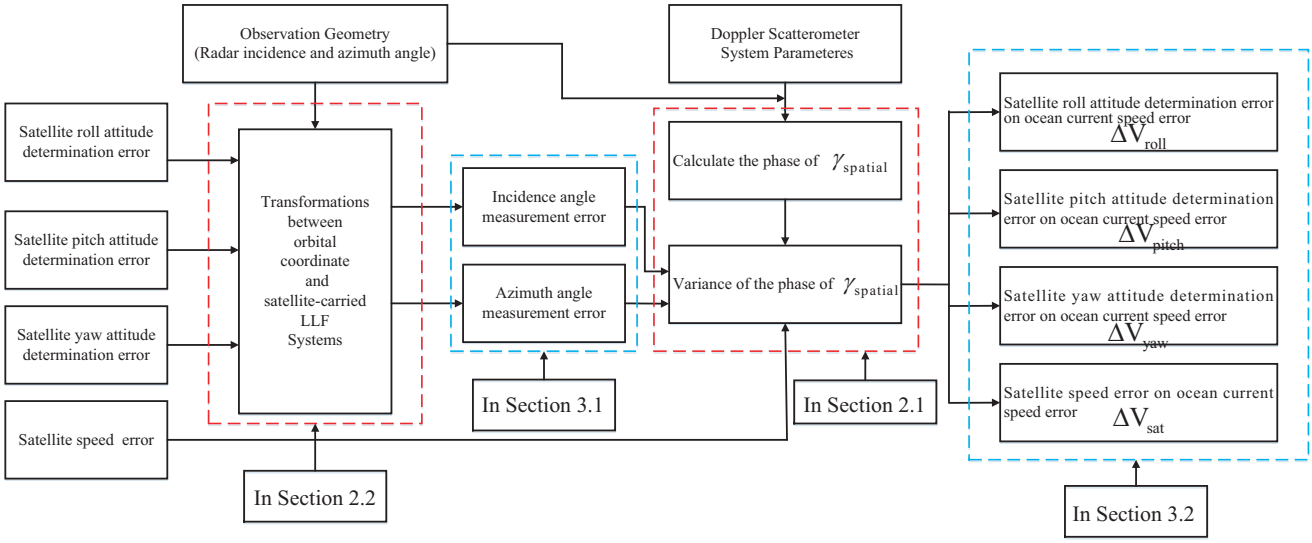

Figure 1. Framework of the methodology adopted in this study. The symbols will be further explained in Section 2 and Section 3.

and speed errors affect ocean current retrieval accuracy, which involves the coherence model and the transformation between orbital coordinate and satellite-carried LFP systems (the red boxes in Figure 1). The coherence model is presented in Section 2.1, and the transformation between orbital coordinate and satellite-carried LFP systems is presented in Section 2.2.

2.1. Coherence Model

The variance of horizontal radial velocity (the surface velocity projected on the ground cell) can be expressed as,

$$\sigma_V = \frac{\lambda}{4\pi\tau \sin\theta}\sigma_\phi, \tag{1}$$

where θ is the radar incidence angle, λ the radar electromagnetic wavelength, τ the time interval ($\tau = 1/PRF$, PRF the pulse repetition frequency in radar system), and σ_ϕ the variance of the interferometric phase ϕ_{int}. Radar measured interferometric phase can be derived from the complex correlation coefficient (γ) of the two consecutive return signals, which writes [18],

$$\phi_{int} = \arg\{\gamma\} \tag{2}$$

We follow the coherence model proposed by Bao et al. [3]. The complex correlation coefficient can be decomposed as the product of four correlation terms, and for the detailed formula derivation the reader is referred to the original paper [3],

$$\gamma = \gamma_{thermal} \cdot \gamma_{footprint} \cdot \gamma_{temporal} \cdot \gamma_{spatial}, \tag{3}$$

where $\gamma_{thermal}$ denotes the thermal noise correlation term, $\gamma_{footprint}$ the correlation term due to different observation regions, $\gamma_{temporal}$ the temporal correlation term, and $\gamma_{spatial}$ the spatial correlation term.

Define that the variances of phases of $\gamma_{temporal}$ and $\gamma_{spatial}$ are σ_{ϕ_t} and σ_{ϕ_s}, respectively, and the variance of the interferometric phase induced by ocean surface current (σ_{ϕ_c}) can be expressed as [3],

$$\sigma_{\phi_c} = \sigma_\phi + \sigma_{\phi_s} + \sigma_{\phi_t}, \tag{4}$$

where σ_ϕ depends on radar system parameters and number of independent samples, and it has been investigated for our proposed Doppler scatterometer [5]. σ_{ϕ_t} is related to the accuracy of Doppler model, which is independent of radar system and is highly dependent on ocean state [13, 14], and σ_{ϕ_s} is dependent on the accuracies of the satellite attitude determination and speed, which will be discussed in details in the following section.

The magnitude of $\gamma_{spatial}$ is determined by several parameters, including radar incidence angle, radar observation azimuth, satellite speed, etc., and it writes [3],

$$\gamma_{spatial} = \frac{\int \exp\left(-j\frac{4\pi}{\lambda}\left(V_{sat}\sin\theta\cos\varphi + V_{earth}\cos\left(\varphi-\varphi_1\right)\right)\tau\right)\operatorname{sinc}\left(\frac{\varphi-\varphi_0}{R_\varphi}\right)^2 d\varphi}{\int \operatorname{sinc}\left(\frac{\varphi-\varphi_0}{R_\varphi}\right)^2 d\varphi}, \tag{5}$$

where V_{sat} is the satellite speed, V_{earth} the speed of the Earth's rotation, φ_1 the angle between V_{sat} and V_{earth}, φ the radar observation azimuth, φ_0 the azimuth at the center of radar footprint, and R_φ the radar resolution in the azimuth direction.

The variance of the phase of $\gamma_{spatial}$ can be expressed as,

$$\sigma_{\phi_s} = \frac{\partial\phi_s}{\partial\theta}\sigma\theta + \frac{\partial\phi_s}{\partial\varphi}\sigma\varphi + \frac{\partial\phi_s}{\partial V_{sat}}\sigma V_{sat}, \tag{6}$$

where ϕ_s is the phase of $\gamma_{spatial}$; $\sigma\theta$, $\sigma\varphi$, and σV_{sat} are the measurement errors of radar incidence angle, radar azimuth, and satellite speed, respectively. These three terms ($\sigma\theta$, $\sigma\varphi$, and σV_{sat}) are induced by errors of satellite attitude determination and speed.

2.2. Transformations between Orbital Coordinate System and Satellite-Carried LLF System

Coordinate frames are used to express the position of a point in relation to some reference, and knowledge of the relationship between reference frames is required for attitude determination. Some useful coordinate frames, satellite-carried LLF coordinate, and orbital coordinate systems are discussed in this section. LLF serves to represent the satellite's attitude and velocity on or near the surface of the Earth [19, 20]. To directly introduce the satellite attitude determinations without other variables, we define our satellite-carried LLF system in Figure 2. The origin (denoted by O) is located at the center of gravity of the flying satellite, with x-axis along with the direction of satellite flying. y-axis is in the right direction of satellite flying, and z-axis points downward to the nadir. Satellite-carried LFP system follows the right-hand rule.

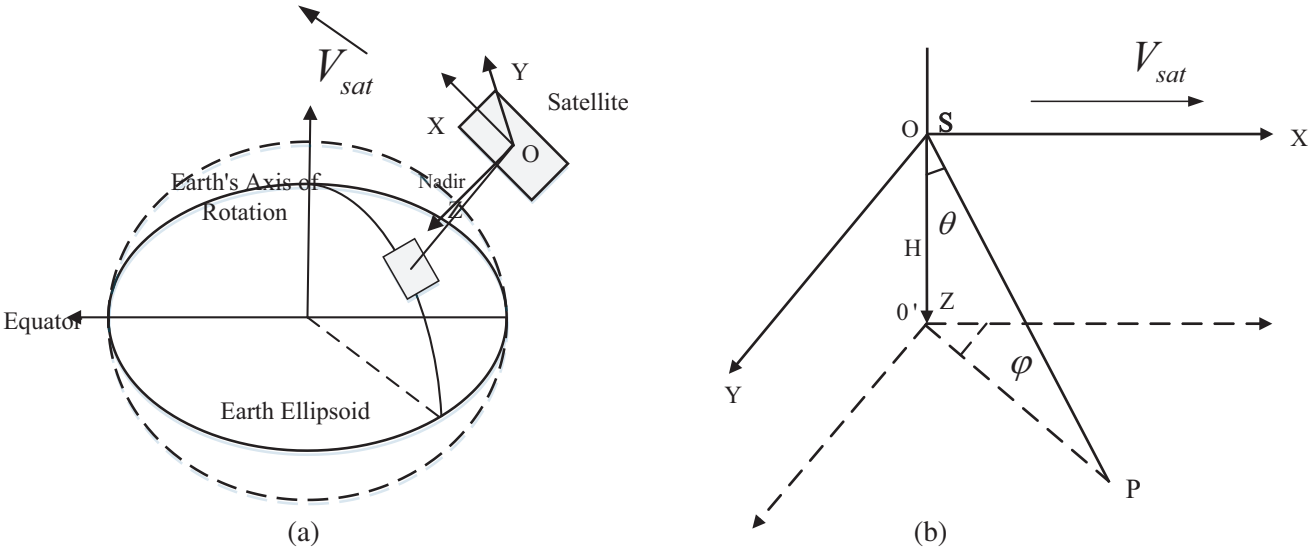

Figure 2. Satellite-carried LLF coordinates, φ is the observation azimuth, θ is the radar incidence angle, H is the height with respect to the observation target, and V_{sat} is satellite speed. (a) With respect to the Earth; (b) Local view of the satellite.

The position of radar is at S point with a coordinate of $(0,0,0)^T$. The coordinate of P point that Doppler scatterometer observes is $(H\tan\theta\cos\varphi, H\tan\theta\sin\varphi, H)^T$. The observation vector with respect to the Doppler scatterometer $\vec{OP}$ writes $\vec{OP} = (H\tan\theta\cos\varphi, H\tan\theta\sin\varphi, H)^T$. The corresponding unit vectors $\vec{OP}_n = (\sin\theta\cos\varphi, \sin\theta\sin\varphi, \cos\theta)^T$, and the unit vector from Doppler scatterometer to the nadir $\vec{n_z}$ is $\vec{n_z} = (0,0,1)^T$.

In space-borne application, the orbital coordinate system has an origin fixed with respect to satellite body, with the roll (x) axis in the nominal direction of the movement of the satellite, the pitch (y) axis out the right-hand side, and the yaw (z) axis such that turning to the right is positive, as illustrated in Figure 3. The origin (denoted by O) is located at the center of gravity of the flying satellite.

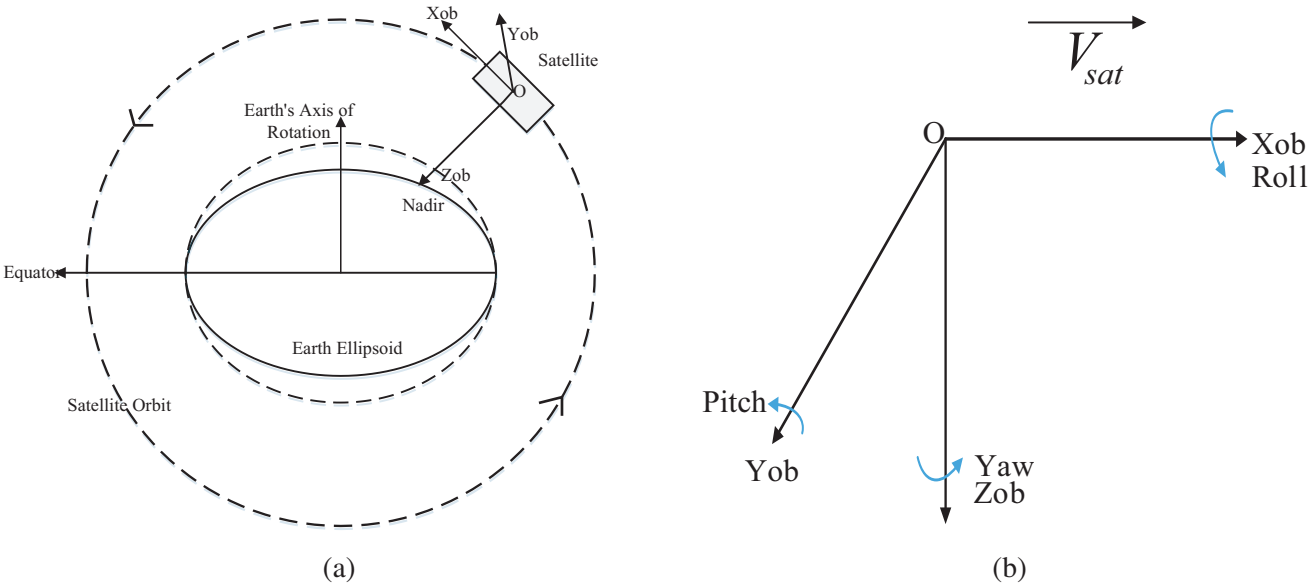

Figure 3. Orbital coordinates system. (a) With respect to the Earth; (b) Local view of the satellite.

In ideal cases, the two coordinates O-X-Y-Z and O-X_{ob}-Y_{ob}-Z_{ob} coincide with each other; however, in actual application, there is an angular deviation on any axis. The angular deviations among corresponding axes are called roll in X-axis, pitch in Y-axis, and yaw in Z-axis. As mentioned earlier, the geometric Doppler shift induced by satellite motion is highly dependent on accurate satellite attitude information, thus, the accuracies of these satellite attitude determination are of great importance on geometric Doppler shift estimates, hence on ocean current retrieval. The orientation of one Cartesian coordinate system with respect to another can always be described by three successive Euler rotations, and the angles of rotation about each of these axes are called Euler angles [21]. Euler angles can be used to define the orientation of one reference frame with respect to another, and a sequence of three rotations is sufficient to describe any transformation.

In this study, the adopted Euler angles move from the reference orbital frame to the satellite-carried LLF frame, following a Z-X-Y (or the so-called 3-1-2) rotation sequence. The first rotation is the yaw about nadir (i.e., satellite z axis); the second rotation is the roll about satellite x axis; and the final rotation is the pitch. The illustration of a Euler rotation is shown in Figure 4.

The unit vector in the X_{ob}-Y_{ob}-Z_{ob} plane can be expressed in terms of angle θ as $(x_{ob}, y_{ob}, z_{ob}) = (\cos\theta, \sin\theta, z_{ob})$, and in the X-Y-Z plane, it can be expressed in terms of angle $\theta - \psi_z$, i.e., $(x, y, z) = (\cos(\theta - \psi_z), \sin(\theta - \psi_z), z)$. ψ_z is the rotation angle about Z_{ob} axis, called yaw. Following the trigonometric identities below,

$$\sin(a \pm b) = \sin a\cos b \pm \cos a\sin b, \tag{7}$$

$$\cos(a \pm b) = \cos a\cos b \mp \sin a\sin b, \tag{8}$$

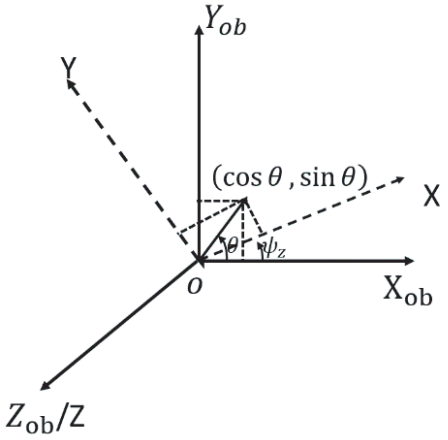

Figure 4. The illustration of Euler rotation, rotation about Z_{ob} axis.

Thus, x and y can be written as,

$$x = \cos\theta\cos\psi_z + \sin\theta\sin\psi_z, \tag{9}$$

$$y = \sin\theta\cos\psi_z - \cos\theta\sin\psi_z, \tag{10}$$

Considering that $z = z_{ob}$, thus the above equations can be expressed in matrix as,

$$\begin{bmatrix} x \\ y \\ z \end{bmatrix} = \begin{bmatrix} \cos\psi_z & \sin\psi_z & 0 \\ -\sin\psi_z & \cos\psi_z & 0 \\ 0 & 0 & 1 \end{bmatrix} \cdot \begin{bmatrix} x_{ob} \\ y_{ob} \\ z_{ob} \end{bmatrix}, \tag{11}$$

$$A_z(\Psi_z) = \begin{bmatrix} \cos\psi_z & \sin\psi_z & 0 \\ -sin\psi_z & \cos\psi_z & 0 \\ 0 & 0 & 1 \end{bmatrix}, \tag{12}$$

where $A_z(\Psi_z)$ is the transformation rotation base around Z_{ob} axis. Similarly, we can get the transformation rotation base around X_{ob} and Y_{ob} axes.

$$A_x(\Psi_x) = \begin{bmatrix} 1 & 0 & 0 \\ 0 & \cos\Psi_x & \sin\Psi_x \\ 0 & -\sin\Psi_x & \cos\Psi_x \end{bmatrix}, \tag{13}$$

$$A_y(\Psi_y) = \begin{bmatrix} \cos\Psi_y & 0 & -\sin\Psi_y \\ 0 & 1 & 0 \\ \sin\Psi_y & 0 & \cos\Psi_y \end{bmatrix}, \tag{14}$$

where Ψ_x and Ψ_y are satellite roll and pitch, respectively.

We use the notation A^{to}_{from} to denote a coordinate transformation matrix from one coordinate frame (designated by "from") to another coordinated frame (designed by "to"). For example, A^{LLF}_{ob} denotes the coordinate transformation matrix from orbital coordinates to satellite-carried LLF coordinates, which combines all the above three rotations by multiplying the cosine matrices into a single transformation matrix, and can be expressed as,

$$\begin{aligned} A^{LLF}_{ob} &= A_y(\Psi_y) \cdot A_x(\Psi_x) \cdot A_z(\Psi_z) \\ &= \begin{bmatrix} \cos\Psi_y\cos\Psi_z - \sin\Psi_y\sin\Psi_x\sin\Psi_z & \cos\Psi_y\sin\Psi_z + \sin\Psi_y\sin\Psi_x\cos\Psi_z & -\sin\Psi_y\cos\Psi_x \\ -\sin\Psi_z\cos\Psi_x & \cos\Psi_x\cos\Psi_z & \sin\Psi_x \\ \cos\Psi_z\sin\Psi_y + \sin\Psi_z\sin\Psi_x\cos\Psi_y & \sin\Psi_y\sin\Psi_z - \cos\Psi_z\sin\Psi_x\cos\Psi_y & \cos\Psi_y\cos\Psi_x \end{bmatrix}. \end{aligned} \tag{15}$$

In turn, the transformation matrix A^{ob}_{LLF} from the satellite-carried LLF system to the orbital coordinate system can be expressed as,

$$A^{ob}_{LLF} = A^{LLF^{-1}}_{ob} = A^{LLF^T}_{ob}, \tag{16}$$

where $A_{ob}^{LLF^{-1}}$ is the inverse matrix of A_{ob}^{LLF}, and $A_{ob}^{LLF^T}$ is the transpose matrix of A_{ob}^{LLF}, since the transformation matrix A_{ob}^{LLF} is orthogonal matrix.

3. EFFECTS OF ACCURACIES OF SATELLITE ATTITUDE DETERMINATIONS AND SPEED ON OCEAN CURRENT RETRIEVAL

In this section, we derive detailed formulas to investigate how satellite attitude determinations affect radar incidence angle and azimuth, and hence on ocean current retrieval. We derive the expressions of the incidence angle and observation azimuth errors induced by satellite attitude determination including roll, pitch, and yaw, respectively, in Section 3.1. Based on this, we investigate the effects of accuracies of satellite attitude determinations and speed on radar incidence angle and observation azimuth. In Section 3.2, we further analyze the effects of accuracies of satellite attitude determinations and speed on ocean current retrieval.

3.1. Effects of Accuracies of Satellite Attitude Determinations on Radar Incidence Angle and Observation Azimuth

The unit vector $O\vec{P}_n$ in the satellite-carried LLF coordinate can be expressed in the orbital coordinates via the transformation matrix A_{LLF}^{ob}, and it writes,

$$O\vec{P}_n^{xyz} = A_{LLF}^{ob} \cdot O\vec{P}_n = A_{ob}^{LLF^T} \cdot (\sin\theta\cos\varphi, \sin\theta\sin\varphi, \cos\theta)^T = \begin{bmatrix} A \\ B \\ C \end{bmatrix}, \quad \text{where} \tag{17}$$

$$\begin{aligned} A &= (\cos\Psi_y\cos\Psi_z - \sin\Psi_y\sin\Psi\varphi_x\sin\Psi_z)\cdot\sin\theta\cos\varphi - \sin\Psi_z\cos\Psi_x\sin\theta\sin\varphi \\ &\quad + \cos\theta\left(\cos\Psi_z\sin\Psi_y + \sin\Psi_z\sin\Psi_x\cos\Psi_y\right), \end{aligned} \tag{18}$$

$$\begin{aligned} B &= (\cos\Psi_y\sin\Psi_z + \sin\Psi_y\sin\Psi_x\cos\Psi_z)\cdot\sin\theta\cos\varphi + \cos\Psi_x \\ &\quad + \cos\theta\left(\sin\Psi_y\sin\Psi_z - \cos\Psi_z\sin\Psi_x\cos\Psi_y\right) \end{aligned} \tag{19}$$

$$C = -\sin\Psi_y\cos\Psi_x\sin\theta\cos\varphi + \sin\Psi_x\sin\theta\sin\varphi + \cos\theta\cos\Psi_y\cos\Psi_x. \tag{20}$$

If $\Psi_y = 0$ and $\Psi_z = 0$, we can get $O\vec{P}_n^x = \begin{bmatrix} \sin\theta\cos\varphi \\ \cos\Psi_x\sin\theta\sin\varphi - \cos\theta\sin\Psi_x \\ \sin\Psi_x\sin\theta\sin\varphi + \cos\theta\cos\Psi_x \end{bmatrix}$.

If $\Psi_x = 0$ and $\Psi_z = 0$, we can get $O\vec{P}_n^y = \begin{bmatrix} \cos\Psi_y\sin\theta\cos\varphi + \cos\theta\sin\Psi_y \\ \sin\theta\sin\varphi \\ -\sin\Psi_y\sin\theta\cos\varphi + \cos\theta\cos\Psi_y \end{bmatrix}$.

If $\Psi_x = 0$ and $\Psi_y = 0$, we can get $O\vec{P}_n^z = \begin{bmatrix} \sin\theta\cos(\varphi + \Psi_z) \\ \sin\theta\sin(\varphi + \Psi_z) \\ +\cos\theta \end{bmatrix}$.

For unit vectors $\vec{I}_a$ and $\vec{I}_b$, the angle between $\vec{I}_a$ and $\vec{I}_b$, θ_{ab} is,

$$\theta_{ab} = \cos^{-1}\left(\vec{I_a}^T \cdot \vec{I}_b\right). \tag{21}$$

When only satellite roll attitude Ψ_x exists, the corresponding incidence angle θ_x and observation azimuth φ_x are,

$$\theta_x = \cos^{-1}\left(\vec{n_z}^T \cdot O\vec{P}_n^x\right) = \cos^{-1}\left(\sin\Psi_x\sin\theta\sin\varphi + \cos\theta\cos\Psi_x\right), \tag{22}$$

$$\varphi_x = \tan^{-1}\left(\frac{O\vec{P}_n^x(2)}{O\vec{P}_n^x(1)}\right) = \tan^{-1}\left(\frac{\cos\Psi_x\sin\theta\sin\varphi - \cos\theta\sin\Psi_x}{\sin\theta\cos\varphi}\right). \tag{23}$$

Similarly, the corresponding incidence angle θ_y and θ_z, observation azimuth φ_y and φ_z induced by Ψ_y and Ψ_z, respectively, can be expressed as,

$$\theta_y = \cos^{-1}\left(\vec{n_z}^T \cdot O\vec{P}_n^y\right) = \cos^{-1}\left(-\sin\Psi_y\sin\theta\cos\varphi + \cos\theta\cos\Psi_y\right), \tag{24}$$

$$\varphi_y = \tan^{-1}\left(\frac{O\vec{P}_n^y(2)}{O\vec{P}_n^y(1)}\right) = \tan^{-1}\left(\frac{\sin\theta\sin\varphi}{\cos\Psi_y\sin\theta\cos\varphi - \cos\theta\sin\Psi_y}\right), \tag{25}$$

$$\theta_z = \cos^{-1}\left(\vec{n_z}^T \cdot \vec{R}_n^z\right) = \theta, \tag{26}$$

$$\varphi_z = \tan^{-1}\left(\frac{O\vec{P}_n^z(2)}{O\vec{P}_n^z(1)}\right) = \tan^{-1}\left(\frac{\sin\theta\cos(\varphi+\Psi_z)}{\sin\theta\cos(\varphi+\Psi_z)}\right) = \varphi + \Psi_z. \tag{27}$$

Therefore, the incidence angle and observation azimuth errors induced by satellite attitude determination can be calculated by,

$$\Delta\theta = \theta_a - \theta, \tag{28}$$

$$\Delta\varphi = \varphi_a - \varphi, \tag{29}$$

where θ_a can be θ_x, θ_y, and θ_z, φ_a can be φ_x, φ_y, and φ_z.

The satellite attitude error is defined as the difference between the true and estimated attitudes. Currently using multi-sensors fusion, an accuracy of satellite attitude determination of 0.001° is achievable in the post-processing [12]. Following the methodology as shown in Figure 1, selecting the satellite attitude determination errors as input, we simulate the incidence angel and observation azimuth errors induced by the errors of satellite roll, pitch, and yaw attitude determinations, and the variations versus azimuths are shown in Figure 5.

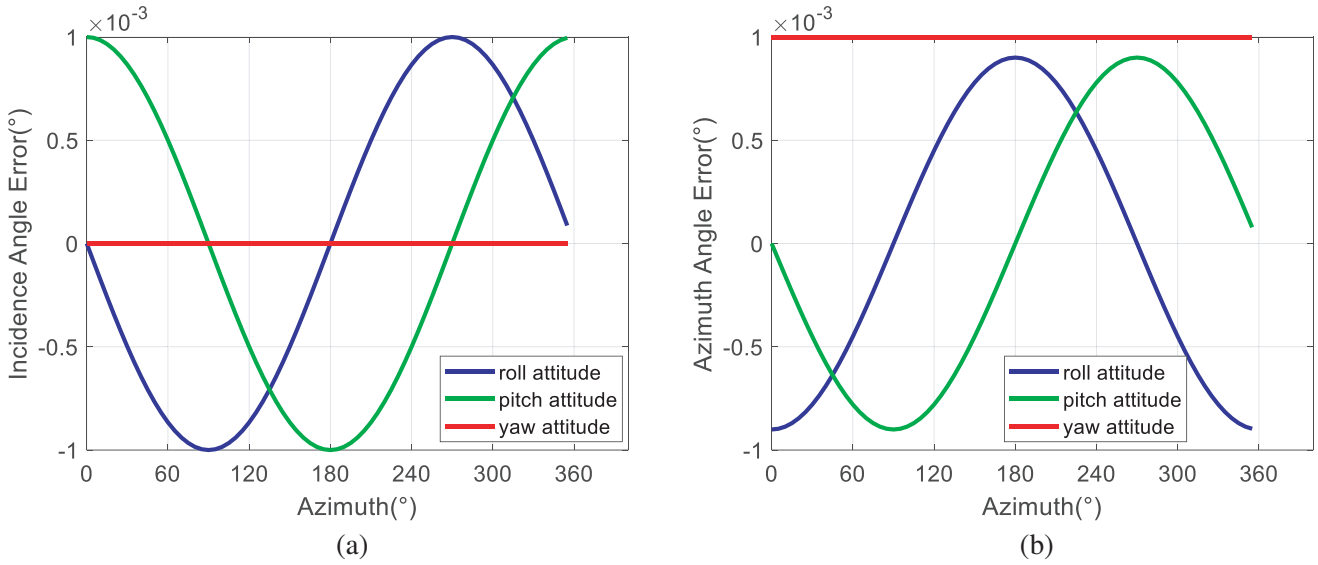

Figure 5. Effects of satellite attitude determinations with an accuracy of 0.001° on incidence angle and observation azimuth errors. (a) Incidence angle errors; (b) Observation azimuth errors.

From Figure 5, it can be found that radar incidence angle is not affected by the satellite yaw determination, while the satellite yaw error has a constant influence on observation azimuth, where the absolute magnitude depends on the accuracy of yaw attitude. In addition, the accuracy of roll determination has the largest effect on radar incidence angle at side-looking direction (i.e., 90° azimuth), while the pitch term has the largest effect at forward and afterward-looking directions (i.e., 0° and 180° azimuth). As for the observation azimuth errors, satellite roll determination follows a cosine-shape variation versus different azimuths and reaches an absolute maximum at forward and afterward-looking directions, while the pitch follows a sine-shape variation and reaches an absolute maximum at side-looking direction. By comparisons, with the same accuracy of satellite attitude determination, the yaw determination has a larger effect on observation azimuth.

3.2. Effects of Accuracies of Satellite Attitude Determination and Speed on Ocean Current Retrieval

Based on Equation (1), the ocean current speed error induced by the accuracies of satellite attitude and speed determinations can be expressed as,

$$\Delta V_{roll} = \frac{\lambda}{4\pi\tau\sin\theta}\left(\frac{\partial\phi_s}{\partial\theta}(\theta_x-\theta)+\frac{\partial\phi_s}{\partial\varphi}(\varphi_x-\varphi)\right), \tag{30}$$

$$\Delta V_{pitch} = \frac{\lambda}{4\pi\tau\sin\theta}\left(\frac{\partial\phi_s}{\partial\theta}(\theta_y-\theta)+\frac{\partial\phi_s}{\partial\varphi}(\varphi_y-\varphi)\right), \tag{31}$$

$$\Delta V_{yaw} = \frac{\lambda}{4\pi\tau\sin\theta}\left(\frac{\partial\phi_s}{\partial\theta}(\theta_z-\theta)+\frac{\partial\phi_s}{\partial\varphi}(\varphi_z-\varphi)\right), \tag{32}$$

$$\Delta V_{sat} = \frac{\lambda}{4\pi\tau\sin\theta}\sigma V_{sat}. \tag{33}$$

where ΔV_{roll} is the ocean current speed error induced by satellite roll attitude accuracy, ΔV_{pitch} for pitch accuracy, ΔV_{yaw} for yaw accuracy, and ΔV_{sat} for satellite speed accuracy.

To calculate the ocean current speed errors induced by the accuracies of satellite attitude and speed, it needs the information of radar incidence angle θ, radar electromagnitude wavelength λ, phase of spatial correlation coefficient, and time interval τ. Based on the above Equations (30)–(33), using the system parameters optimized in [12], i.e., $\tau = 1/16$ kHz at the orbital height of 520 km with an incidence angle of 48° at Ka-band (the related parameters are shown in Table 1), we investigate the

Table 1. Parameters used in this study.

Parameters	Value
Carrier Frequency of Doppler scatterometer	35.75 GHz
Carrier wavelength	0.84 cm
Incidence angle	48°
PRF	16 kHz
3 dB azimuth beamwidth	0.42°
3 dB range beamwidth	0.42°
Satellite orbital height	520 km
Satellite velocity	7606 m/s

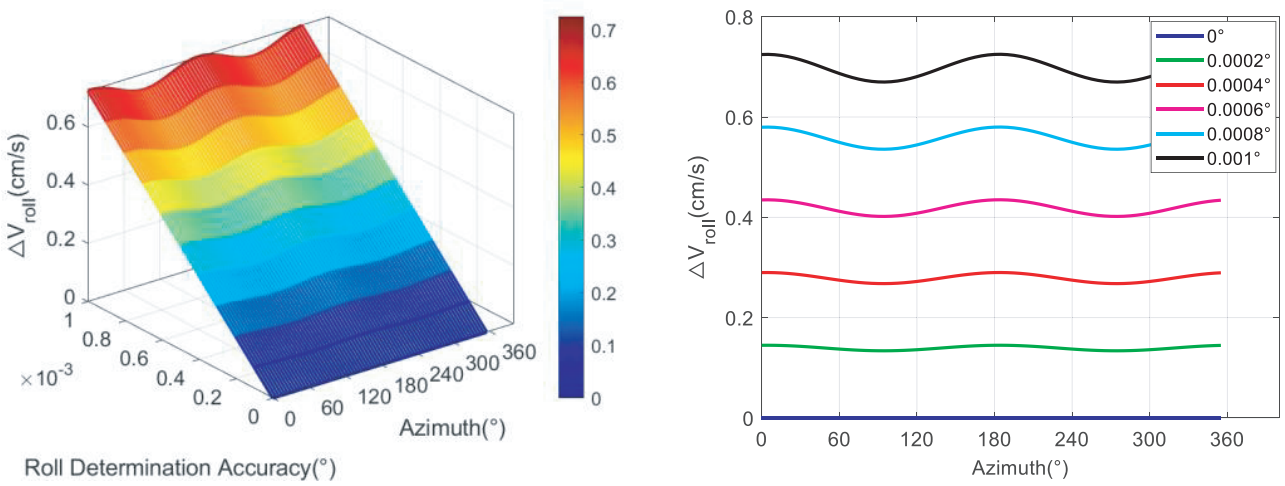

(a) (b)

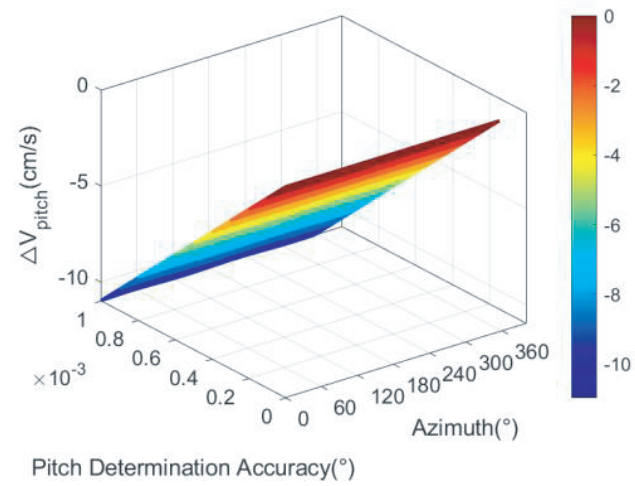

(c)

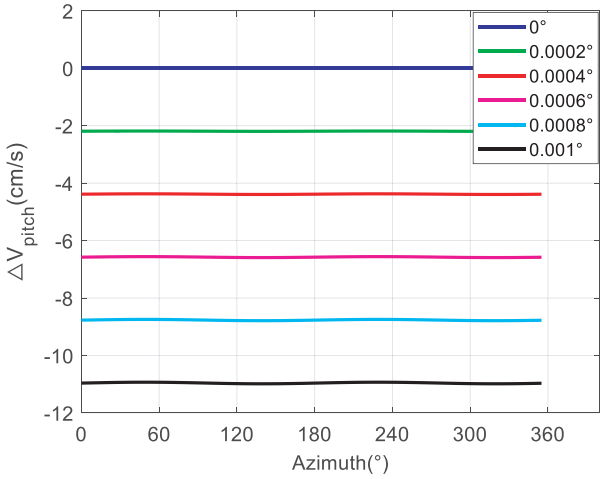

(d)

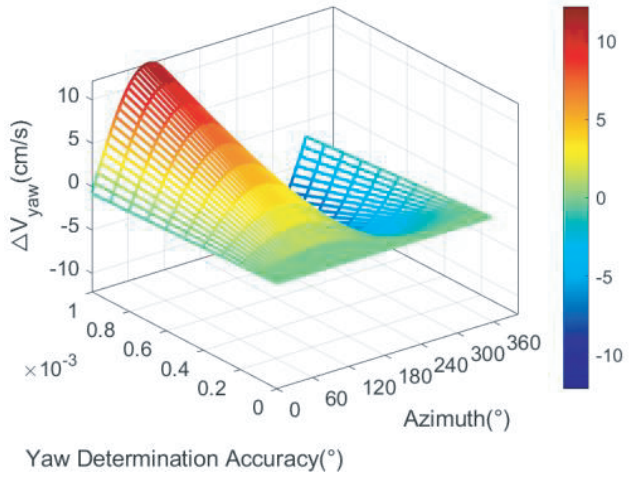

(e)

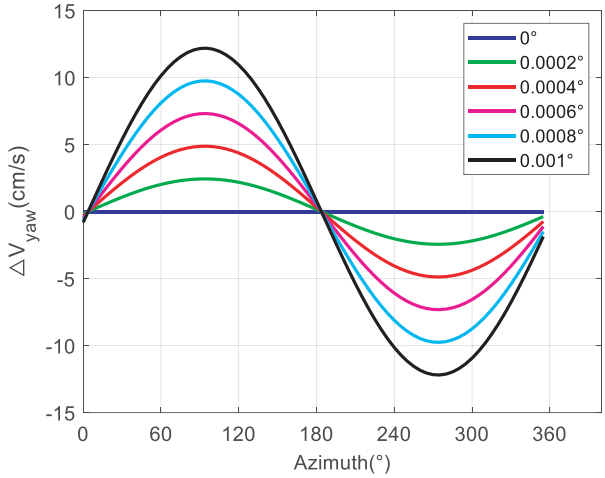

(f)

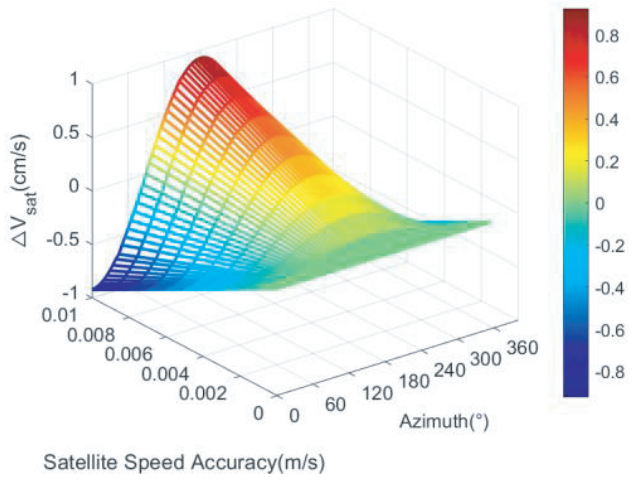

(g)

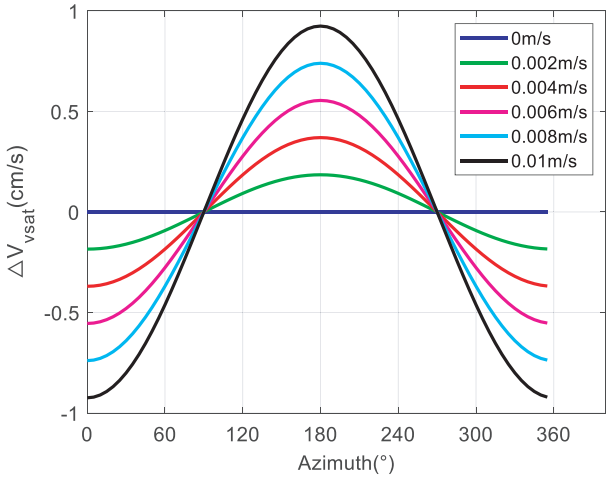

(h)

Figure 6. Effects of satellite attitude determination and speed errors on ocean current retrieval. (a)–(b) Roll determination accuracy; (c)–(d) Pitch determination accuracy; (e)–(f) Yaw determination accuracy; (g)–(h) Satellite speed accuracy.

variations of ocean current speed errors induced by satellite attitude determinations and speed errors.

As shown in Figure 6, given an azimuth, the variance of ocean current speed increases with the increasing errors of satellite attitude determinations and speed. Comparing the absolute magnitudes of ΔV_{roll}, ΔV_{pitch}, and ΔV_{yaw}, it can be found that the variance of ocean current speed induced by roll determination error is the smallest, less than 0.8 cm/s. ΔV_{sat} has the minimum absolute magnitude at 90° azimuth (i.e., at side-looking view), and the maximum absolute magnitude occurs at 0° and 180° (i.e., at forward and backward-looking directions). With a satellite speed accuracy of 0.01 m/s, the maximum ocean current speed error induced by satellite speed error is less than 1 cm/s.

The satellite attitude determinations (including roll, pitch, and yaw) and satellite speed errors are independent random variables, and the total ocean current speed error induced by satellite attitude determinations and speed errors can be expressed as,

$$\Delta V_t = \sqrt{(\Delta V_{roll})^2 + (\Delta V_{pitch})^2 + (\Delta V_{yaw})^2 + (\Delta V_{sat})^2}. \tag{34}$$

The variations of ΔV_t versus azimuths and accuracies of attitude determination are shown in Figure 7.

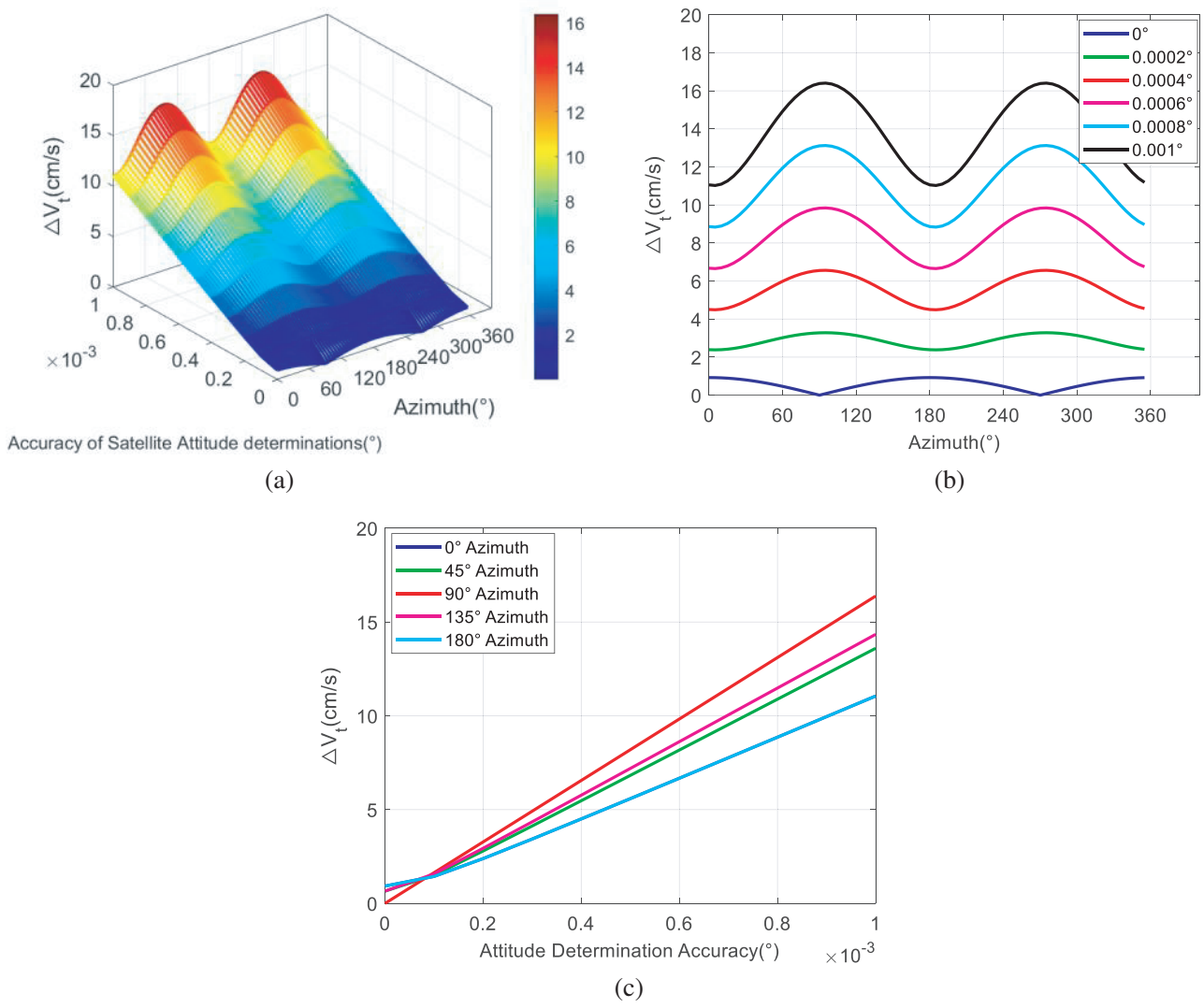

Figure 7. The total ocean current error induced by accuracies of satellite attitude determination with a speed error of 0.01 m/s: (a) 3-D plots at different accuracies versus azimuths; (b) 2-D plots at different azimuths, with an attitude accuracy step of 0.0002°; (c) 2-D plots versus different accuracies of satellite attitude at different azimuths.

As shown in Figure 7, the total ocean current speed error, ΔV_t, induced by satellite attitude and speed errors increases linearly with the increasing satellite attitude errors. When no attitude errors exist, ΔV_t is determined by the satellite speed error, and the maximum magnitude of ΔV_t is less than 1 cm/s, which is negligible and can be ignored in the practical application. However, in the practical application, there will be inevitably satellite attitude errors, with an attitude accuracy of 0.001°. ΔV_t reaches a maximum value of 16.37 cm/s at 90° azimuth and a minimum value of 11.05 cm/s at forward and backward-looking directions.

4. SUMMARY AND CONCLUSIONS

From the perspective of ocean current retrieval, ocean current retrieval accuracy is determined by the accuracies of interferometric phase estimation of the radar system, wind-wave induced Doppler shift estimation, and satellite motion induced Doppler shift estimation, and the first two issues have been carefully investigated in [5, 13]. In this study, we focus on the effects of accuracy of satellite motion induced Doppler shift estimation on ocean current. The accurate satellite motion induced Doppler shift estimation is tied up with accuracies of satellite attitude determination and speed, thus the satellite attitude determination and speed errors would inevitably affect the ocean current retrieval.

In this study, we derive detailed formulas to investigate how satellite attitude determination and speed errors affect ocean current retrieval for a Doppler scatterometer, which involves the spatial correlation coefficient phase and the transformation between orbital coordinate and satellite-carried LFP systems. Our results show that satellite attitude errors including roll, pitch, and yaw would introduce errors in radar incidence angle and observation azimuth, and hence on ocean current retrieval. It has been found that the error of satellite yaw determination has no impact on radar incidence angle, while it has a constant impact on observation azimuth, whose magnitude depends on the satellite yaw determination accuracy. The satellite roll determination error has the largest effect on radar incidence angle at side-looking direction while the pitch term has the largest impact at forward and afterward-looking direction. In addition, the ocean current speed error induced by errors of satellite attitude determination and speed is highly associated with the specific radar system parameters. For our Ka-band Doppler scatterometer system with a $PRF = 16$ kHz and an incidence angle of 48° at the orbital height of 520 km, for a 0.001° attitude accuracy, the maximum magnitude of ocean current speed error is less than 0.8 cm/s for the roll-induced, then is the pitch-induced around 10.93 cm/s and followed by the yaw-induced around 12.16 cm/s at side-looking direction. Compared with the satellite yaw and pitch determination errors, ocean current speed error induced by roll determination error is the smallest. Furthermore, compared with satellite attitude determination error, satellite speed error has a relatively smaller impact on ocean current retrieval. With a speed error of 0.01 m/s, the corresponding ocean current speed error induced by satellite speed error is less than 1 cm/s, which is negligible.

Considering that satellite attitude determination (including roll, pitch, and yaw) and speed errors are independent random errors, the total ocean current speed error induced by satellite attitude and speed errors can be expressed in the form of the sum of squares of these four terms and then make a square. With a satellite attitude accuracy of 0.001° and a speed accuracy of 0.01 m/s, the total ocean current speed error induced by satellite attitude and speed errors reaches a maximum value of 16.37 cm/s at side-looking direction and reaches a minimum value of 11.05 cm/s at forward and backward-looking directions. While this is a larger value than desired, the accurate correction of bias induced by satellite attitude determination and speed errors is tied up with the post-processing data processing.

Our study indicates the great importance of satellite attitude and speed accuracies on ocean current retrieval for the future ocean current mission and will also be useful to motivate the design of future Doppler measurement instruments.

REFERENCES

1. Song, X., "The importance of including sea surface current when estimating air-sea turbulent heat fluxes and wind stress in the gulf stream region," *Journal of Atmospheric and Oceanic Technology*, Vol. 38, No. 1, 119–138, 2021.

2. Shi, Q. and M. A. Bourassa, "Coupling ocean currents and waves with wind stress over the gulf stream," *Remote Sensing*, Vol. 11, No. 12, 1476, 2019. [Online]. Available: https://www.mdpi.com/2072-4292/11/12/1476.
3. Bao, Q., X. Dong, D. Zhu, S. Lang, and X. Xu, "The feasibility of ocean surface current measurement using pencil-beam rotating scatterometer," *IEEE Journal of Selected Topics in Applied Earth Observations and Remote Sensing*, Vol. 8, No. 7, 3441–3451, 2015, doi: 10.1109/JSTARS.2015.2414451.
4. Rodriguez, E., et al., "Estimating ocean vector winds and currents using a Ka-band pencil-beam doppler scatterometer," *Remote Sensing*, Vol. 10, 576, 2018, doi: 10.3390/rs10040576.
5. Miao, Y., X. Dong, Q. Bao, and D. Zhu, "Perspective of a Ku-Ka dual-frequency scatterometer for simultaneous wide-swath ocean surface wind and current measurement," *Remote Sensing*, Vol. 10, 1042, 2018, doi: 10.3390/rs10071042.
6. Ardhuin, F., et al., "Measuring currents, ice drift, and waves from space: The Sea surface KInematics Multiscale monitoring (SKIM) concept," *Ocean Sci.*, Vol. 14, No. 3, 337–354, 2018, doi: 10.5194/os-14-337-2018.
7. Rodríguez, E., M. Bourassa, D. Chelton, J. T. Farrar, D. Long, D. Perkovic-Martin, and R. Samelson, "The winds and currents mission concept," *Frontiers in Marine Science*, Vol. 6, 438, 2019.
8. Du, Y., X. Dong, X. Jiang, Y. Zhang, and S. Peng, "Ocean Surface Current Multiscale Observation Mission (OSCOM): Simultaneous measurement of ocean surface current, vector wind, and temperature," *Progress In Oceanography*, Vol. 193, No. 3, 102531, 2021.
9. Chapron, B., F. Collard, and F. Ardhuin, "Direct measurements of ocean surface velocity from space: Interpretation and validation," *Journal of Geophysical Research: Oceans*, Vol. 110, C7, 2005, doi: 10.1029/2004JC002809.
10. Mouche, A. A., F. Collard, B. Chapron, K. Dagestad, G. Guitton, J. A. Johannessen, V. Kerbaol, and M. W. Hansen, "On the use of doppler shift for sea surface wind retrieval from SAR," *IEEE Transactions on Geoscience and Remote Sensing*, Vol. 50, No. 7, 2901–2909, 2012, doi: 10.1109/TGRS.2011.2174998.
11. Yurovsky, Y., V. Kudryavtsev, S. A. Grodsky, and B. Chapron, "Sea surface Ka-band doppler measurements: Analysis and model development," *Remote. Sens.*, Vol. 11, 839, 2019.
12. Miao, Y., X. Dong, M. A. Bourassa, and D. Zhu, "Effects of different wave spectra on wind-wave induced doppler shift estimates," *IGARSS 2020 — 2020 IEEE International Geoscience and Remote Sensing Symposium*, 5705–5708, IEEE, 2020.
13. Miao, Y., X. Dong, M. A. Bourassa, and D. Zhu, "Effects of ocean wave directional spectra on doppler retrievals of ocean surface current," *IEEE Transactions on Geoscience and Remote Sensing*, 2021.
14. Elyouncha, A., L. E. B. Eriksson, R. Romeiser, and L. M. H. Ulander, "Measurements of sea surface currents in the baltic sea region using spaceborne along-track InSAR," *IEEE Transactions on Geoscience and Remote Sensing*, Vol. 57, No. 11, 8584–8599, 2019, doi: 10.1109/TGRS.2019.2921705.
15. Hansen, M. W., F. Collard, K.-F. Dagestad, J. A. Johannessen, P. Fabry, and B. Chapron, "Retrieval of sea surface range velocities from Envisat ASAR Doppler centroid measurements," *IEEE Transactions on Geoscience and Remote Sensing*, Vol. 49, No. 10, 3582–3592, 2011.
16. Bolandi, H., M. Haghparast, F. Saberi, B. Vaghei, and S. Smailzadeh, "Satellite attitude determination and contol," *Measurement and Control*, Vol. 45, No. 5, 151–157, 2012.
17. Bao, Q., M. Lin, Y. Zhang, X. Dong, S. Lang, and P. Gong, "Ocean surface current inversion method for a doppler scatterometer," *IEEE Transactions on Geoscience and Remote Sensing*, Vol. 55, No. 11, 6505–6516, 2017.
18. Bamler, R. and P. Hartl, "Synthetic aperture radar interferometry," *Inverse Problems*, Vol. 14, No. 4, R1, 1998.
19. Grewal, M. S., A. P. Andrews, and C. G. Bartone, *Global Navigation Satellite Systems, Inertial Navigation, and Integration*, John Wiley & Sons, 2020.

20. Noureldin, A., T. B. Karamat, and J. Georgy, *Fundamentals of Inertial Navigation, Satellite-based Positioning and Their Integration*, 2013.
21. Howley, B., "AA236: Overview of spacecraft attitude determination and control," Lockheed Martin Space Systems Company, 2005.